

Electronic properties of twisted armchair graphene nanoribbons

Arta Sadrzadeh, Ming Hua, and Boris I. Yakobson^{a)}

Department of Mechanical Engineering and Materials Science and Department of Chemistry, Rice University, Houston, Texas 77251, USA

(Received 22 March 2011; accepted 10 June 2011; published online 5 July 2011)

We study the effect of twist on the electronic structure of H-terminated armchair graphene nanoribbons, for both relaxed and unrelaxed unit cell size. We investigate the band gap change as a function of the twist angle for different ribbon widths. In the case of unrelaxed unit cell size, the band gap closes for smaller twist angles as opposed to relaxed unit cell size. We calculate strain energy as a function of twist angle and show its direct correlation with the reduction of the band gap. Furthermore, the conductance is calculated at arbitrary degree of torsion. © 2011 American Institute of Physics. [doi:10.1063/1.3606553]

Since the isolation of graphene sheets by mechanical exfoliation of pyrolytic graphite,¹ there has been numerous studies on electronic and mechanical properties of graphene (for a review, see Ref. 2 for instance). Because of its very high charge carrier mobility,^{1,3,4} graphene has opened up great possibilities in electronic device applications.

Graphene nanoribbons (GNRs) are quasi one dimensional cuts of graphene. They can form zigzag, armchair, or chiral edge patterns. Atoms along the edge of a zigzag GNR (ZGNR) come from the same sublattice of graphene, whereas atoms from two different sublattices form bonds along the edge of an armchair GNR (AGNR).

GNRs have been studied extensively.^{5–8} Hydrogen terminated ZGNRs have ferromagnetic spin ordering along each edge and antiparallel spins for opposite edges.⁵ There are different techniques for synthesizing GNRs; Scanning Tunneling Microscope tip etching,⁹ metallic nanoparticle atomically precise etching,¹⁰ and unzipping carbon nanotubes,¹¹ to name a few.

It has been shown that all hydrogen terminated GNRs are semiconducting, with the band gap gradually going to zero for large widths.⁵ Detailed electronic properties of GNRs vary with the edge pattern. AGNRs fall into three families, depending on their width. With N being the number of dimer lines in an AGNR, these families are $N = 3p - 1$, $3p$, and $3p + 1$, where “ p ” is a positive integer. According to local density approximation calculations, the $N = 3p - 1$ family has narrow band gap.⁵ The gap is inversely proportional to the width in all three families.

In this letter, we present our results for the change in electronic structure caused by a twist in the ribbon.¹² We studied the $N = 3p - 1$ and $N = 3p + 1$ families of AGNRs, optimized their geometric configurations and calculated their band structure using Density Functional Theory (DFT)-based tight binding method¹³ and helical symmetry.^{14,15} As will be shown later, in both families of ribbons, the band gap closes at some certain twist angle. This can be useful in some applications such as switches and sensors. For the $N = 3p$ family, the band gap does not close as a result of twist,¹⁶ and for this reason, it is not considered here. Also, ZGNRs are not considered

since spin polarized calculations are needed for correct accounting of the ferromagnetic edge states, which are not included in our tight binding scheme. It should be mentioned that if the edges are not H-terminated, the twist will be spontaneous.¹⁷

The use of helical symmetry is due to the fact that traditional unit cells for small twist angles become unlimitedly large and the computations become unfeasible. The program used is the Trocadero code^{18,19} with helical symmetry implemented.²⁰ The structures of flat hydrogen terminated GNRs are relaxed until the total energy reduction between steps is less than 3×10^{-5} eV. The unit cell sizes of the flat GNRs are varied until the size with lowest energy is found, to the precision of 3×10^{-4} eV. Twisted GNR structures are relaxed similarly, using the unit cell size of the flat GNRs in the case of unrelaxed unit cell, or optimized individually in the case of relaxed unit cell.

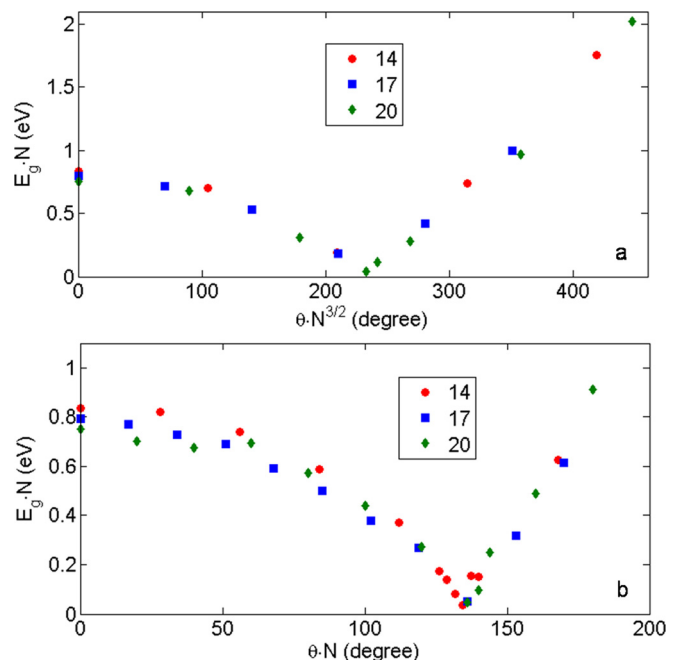


FIG. 1. (Color online) The scaled band gap as a function of scaled twist angle, for (a) unrelaxed unit cell size or (b) relaxed unit cell size, for $N = 14, 17, 20$ AGNRs.

^{a)} Author to whom correspondence should be addressed. Electronic mail: biy@rice.edu.

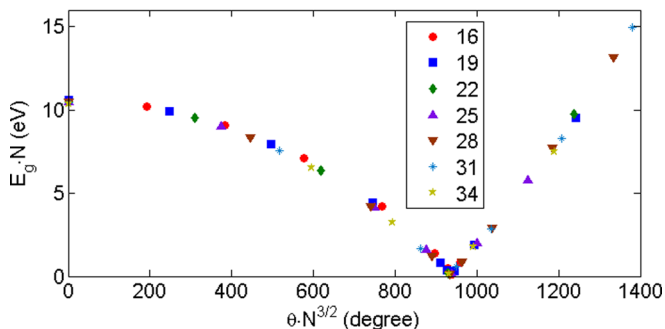


FIG. 2. (Color online) The scaled band gap as a function of scaled twist angle for unrelaxed unit cell size, for $N=16, 19, 22, 25, 28, 31,$ and 34 AGNRs.

The $N=3p-1$ is the narrow band gap case. It has been shown that the band gap closes with twist.¹⁵ We consider relaxed and unrelaxed unit cell size for $N=14, 17,$ and 20 (Ref. 16 only considers the case where the unit cell size is fixed/unrelaxed). For unrelaxed unit cell size, the band gap closing angle (per unit cell) scales as $N^{-3/2}$. This is in agreement with Ref. 16 estimate. The band gap of the flat ribbon scales approximately as N^{-1} . Fig. 1(a) shows the scaled band gap E_g (eV) as a function of the scaled twist angle θ (degrees/unit cell) for all considered cases.

In the relaxed unit cell size case, the scaling is different. We obtained N^{-1} scaling for the band gap closing angle. Fig. 1(b) illustrates the behavior of the band gap as a function of the twist angle for all three widths considered.

For the $N=3p+1$ family also, the band gap closes with twist.¹⁶ For this family of AGNRs, for unrelaxed case, we examined the band gap as a function of the twist angle for $N=16, 19, 22, 25, 28, 31,$ and 34 . The scaling of $N^{-3/2}$ for the band gap closing angle and N^{-1} for the flat ribbon band gap applies here too. Fig. 2 shows the scaled band gap as a function of the scaled twist angle for all considered cases.

For this family of AGNRs, for the relaxed unit cell size case, the band gap decreases with twist but does not close at even large twist angles (more than 15° /unit cell). At such

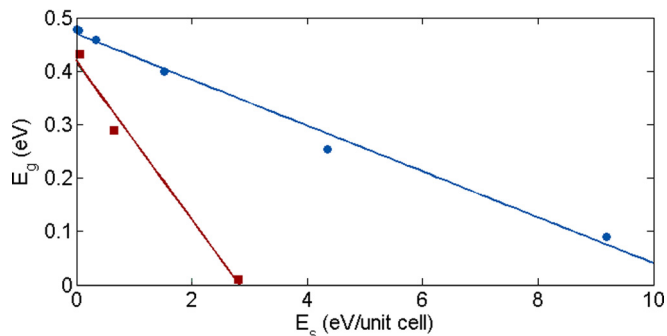


FIG. 4. (Color online) Band gap vs. strain energy for unrelaxed (red/squares) and relaxed (blue/circles) $N=22$ AGNR.

large twist angles, the C-C bonds at the edge of the ribbon break. For this reason, we do not observe band gap closing.

Now, we turn our attention to energies of these structures. We calculated the strain energy per unit length (E_s/L , where L is the relaxed or unrelaxed unit cell length) as a function of the twist angle per unit length (θ/L). Fig. 3 shows the plot. We obtain $E_s \sim \theta^{3.4}$ for $N=22$. This is obviously out of the linear elastic regime, for which we expect a $\sim \theta^4$ relationship. Linear regime is defined by $(\theta/L)*w \ll 1$, where w is the width of GNR. In this case, the linear regime criterion is violated (for the smallest twist angle, we have $(\theta/L)*w=0.32$).

We also studied the band gap as a function of strain energy. It turns out that the band gap change is proportional to the strain energy. This is due to the fact that the bigger band gap change, the bigger change in the energy levels, and consequently, the total energy. The opposite is not necessarily true (we can have zero band gap that does not change with strain). Fig. 4 illustrates the results for $N=22$ AGNR. The plot shows a close to linear relationship between the strain energy and band gap.

It should be mentioned that in the relaxed unit cell size case, at some certain twist angle, the ribbon may go off-axis. This is not the case when the unit cell size is fixed to the

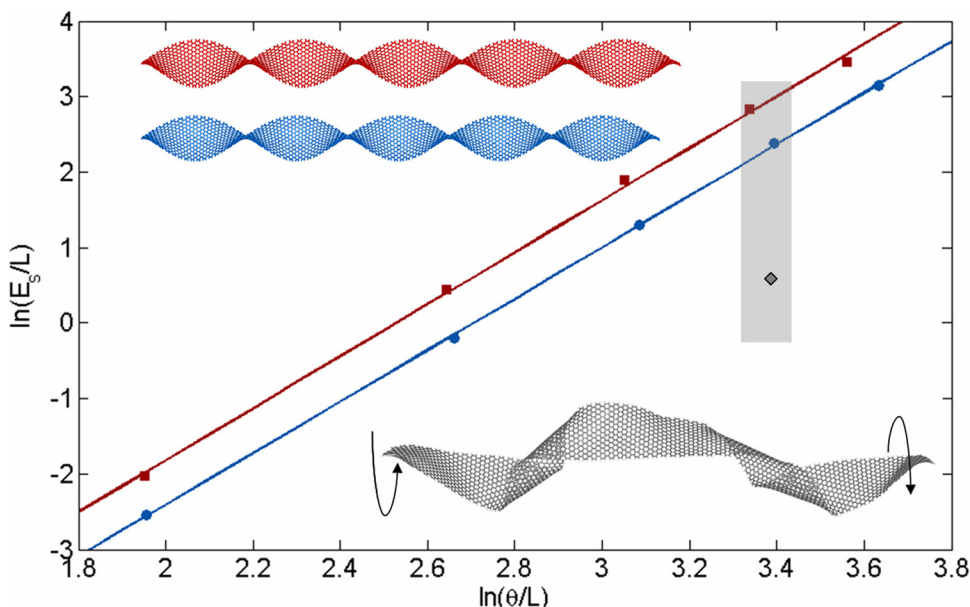


FIG. 3. (Color online) Logarithm of strain energy per unit length (E_s/L) as a function of logarithm of the twist angle per unit length (θ/L) for $N=22$ AGNR. The red/top (blue/bottom) plot/ribbons correspond to unrelaxed (relaxed) unit cell size. The grey/warped ribbon and its energy (grey/diamond) shows the instability of the ribbon for relatively large twists (see text). The slopes of the curves give the $E_s \sim \theta^{3.4}$ power.

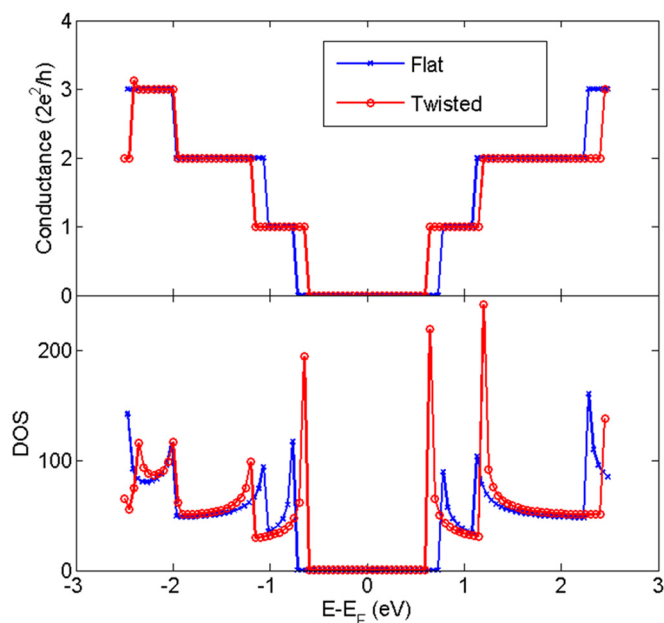


FIG. 5. (Color online) Conductance (top) and density of states (bottom) of flat (blue/dark) and twisted (red/light) ribbon around Fermi level. The steps in conductance plot correspond to van Hove singularities of DOS.

value for the flat ribbon, because the tension keeps the ribbon straight. Using helical symmetry, one can not detect such instability, since each unit cell is a replica of the previous unit cell with twist and translation along the axis. But since we are interested in the band structure of the twisted ribbons, we limit ourselves to helically symmetric regime and do not consider such deformations. We note that for small twist angles, such instability does not occur, and the critical twist angle at which the ribbon bends off-axis is smaller for wider ribbons.

Finally, we calculated conductance of flat and $\theta = 30^\circ$ /unit cell twisted $N = 7$ AGNR around Fermi level, using nonequilibrium Green function formulation.²¹ The results for conductance and density of states (DOS) are shown in Fig. 5. As mentioned before, for the twisted ribbon, traditional unit cell can be quite large. Usually one uses the traditional unit cells (translationally symmetric) as building blocks for the principle layer for conductance calculations. A principle layer consists of the minimum number of unit cells so that each layer only interacts with the nearest neighboring layers. Applying helical symmetry, we choose the principle layer for conductance calculation to be much smaller than traditional unit cell (only 3 ribbon unit cells, where traditional unit cell for $\theta = 30^\circ$ /unit cell consists of 12 ribbon cells, and can be unlimitedly large for small twist angles). We have verified that using this reduced unit cell as principle layer, we obtain the same results for conductance as using traditional unit cell. The critical point is that the Hamiltonian and overlap matrices should be invariant under the symmetry transformation. This requires that the p orbitals (in a 4 or

bital/carbon tight binding approximation) be rotated under a helical symmetry transformation. For this reason, this does not work in usual atomic based DFT basis, where the basis does not rotate under helical transformation.

In conclusion, we studied the change in electronic structure of two families of AGNRs; $N = 3p - 1$ and $N = 3p + 1$, as a result of twist around the axis. The band gap closes at a certain twist angle which scales as $N^{-3/2}$ for unrelaxed and as N^{-1} for relaxed unit cell size. This can be useful for switches or sensors applications. We find a simple linear relationship between band gap and strain energy. We also investigated into the dependence of conductance and DOS on energy of carriers with or without twist. We finally note that temperature removes the effects of spin polarization in ZGNR, rendering the tight binding approximation applicable, which reveals no band gap sensitivity to torsion.

We would like to thank A. Dobrinsky for useful discussions and K. Bets for her help. This work was supported by the Air Force Research Laboratory and by the Welch Foundation (C-1590).

- ¹K. S. Novoselov, A. K. Geim, S. V. Morozov, D. Jiang, Y. Zhang, S. V. Dubonos, I. V. Grigorieva, and A. A. Firsov, *Science* **306**, 666 (2004).
- ²S. Dutta and S. K. Pati, *J. Mater. Chem.* **20**, 8207 (2010).
- ³K. S. Novoselov, D. Jiang, F. Schedin, T. J. Booth, W. Khotkevich, S. V. Morozov, and A. K. Geim, *Proc. Natl. Acad. Sci. U.S.A.* **102**, 10451 (2005).
- ⁴K. S. Novoselov, A. K. Geim, S. V. Morozov, D. Jiang, M. I. Katsnelson, I. V. Grigorieva, S. V. Dubonos, and A. A. Firsov, *Nature* **438**, 197 (2005).
- ⁵Y.-W. Son, M. L. Cohen, and S. G. Louie, *Phys. Rev. Lett.* **97**, 216803 (2006).
- ⁶K. Nakada, M. Fujita, G. Dresselhaus, and M. S. Dresselhaus, *Phys. Rev. B* **54**, 17954 (1996).
- ⁷S. Okada and A. Oshiyama, *Phys. Rev. Lett.* **87**, 146803 (2001).
- ⁸D. A. Abanin, P. A. Lee, and L. S. Levitov, *Phys. Rev. Lett.* **96**, 176803 (2006).
- ⁹L. Tapasztó, G. Dobrik, P. Lambin, and L. P. Biro, *Nat. Nanotechnol.* **3**, 397 (2008).
- ¹⁰S. S. Datta, D. R. Strachan, S. M. Khamis, and A. T. C. Johnson, *Nano Lett.* **8**, 1912 (2008).
- ¹¹D. V. Kosynkin, A. L. Higginbotham, A. Sinitskii, J. R. Lomeda, A. Dimiev, B. K. Price, and J. M. Tour, *Nature* **458**, 872 (2009).
- ¹²A. Dobrinsky, A. Sadrzadeh, J. Xu, and B. I. Yakobson, *Int. J. High Speed Electron. Syst.* **20**, 153 (2011).
- ¹³D. Porezag, T. Frauenheim, T. Köller, G. Seifert, and R. Kashner, *Phys. Rev. B* **51**, 12947 (1995).
- ¹⁴C. T. White, D. H. Robertson, and J. W. Mintmire, *Phys. Rev. B* **47**(9), R5485 (1993).
- ¹⁵P. Koskinen and O. O. Kit, *Phys. Rev. Lett.* **105**, 106401 (2010).
- ¹⁶D. Gunlycke, J. Li, J. W. Mintmire, and C. T. White, *Nano Lett.* **10**, 3638 (2010).
- ¹⁷K. V. Bets and B. I. Yakobson, *Nano Res.* **2**, 161 (2009).
- ¹⁸R. Rurali and E. Hernandez, *Comput. Mater. Sci.* **28**, 85 (2003).
- ¹⁹D.-B. Zhang, M. Hua, and T. Dumitrica, *J. Chem. Phys.* **128**, 084104 (2008).
- ²⁰T. Dumitrica and R. D. James, *J. Mech. Phys. Solids* **55**, 2206 (2007).
- ²¹S. Datta, *Electron Transport in Mesoscopic Systems* (Cambridge University Press, Cambridge, 1995).